



Coupled CO₂ and O₂-driven compromises to marine life in summer along the Chilean sector of the Humboldt Current System

E. Mayol^{1,2}, S. Ruiz-Halpern², C. M. Duarte^{1,3}, J. C. Castilla^{1,4}, and J. L. Pelegrí^{1,5}

¹Laboratorio Internacional de Cambio Global, CSIC-PUC, Facultad de Ciencias Biológicas, Edificio No. 210, Of. 425, Pontificia Universidad Católica de Chile, Avenida Bernardo O'Higgins 340 ó Portugal 49, Santiago, Casilla 114-D, Chile

²Instituto Mediterráneo de Estudios Avanzados, CSIC-UIB, Miquel Marqués 21, 07190 Esporles, Mallorca, Spain

³The UWA Oceans Institute, University of Western Australia, 35 Stirling Highway, Crawley 6009, Australia

⁴Departamento de Ecología, Facultad de Ciencias Biológicas, Pontificia Universidad Católica de Chile, Alameda 340, Santiago, Chile

⁵Institut de Ciències del Mar, CSIC, Barcelona, Spain

Correspondence to: E. Mayol (emayol@imedea.uib-csic.es)

Received: 22 October 2010 – Published in Biogeosciences Discuss.: 6 December 2010

Revised: 9 February 2012 – Accepted: 20 February 2012 – Published: 28 March 2012

Abstract. Carbon dioxide and coupled CO₂ and O₂-driven compromises to marine life were examined along the Chilean sector of the Humboldt Current System, a particularly vulnerable hypoxic and upwelling area, applying the Respiration index ($RI = \log_{10} \frac{pO_2}{pCO_2}$) and the pH-dependent aragonite saturation (Ω) to delineate the water masses where aerobic and calcifying organisms are stressed. As expected, there was a strong negative relationship between oxygen concentration and pH or pCO_2 in the studied area, with the subsurface hypoxic Equatorial Subsurface Waters extending from 100 m to about 300 m depth and supporting elevated pCO_2 values. The lowest RI values, associated to aerobic stress, were found at about 200 m depth and decreased towards the Equator. Increased pCO_2 in the hypoxic water layer reduced the RI values by as much as 0.59 RI units, with the thickness of the upper water layer that presents conditions suitable for aerobic life ($RI > 0.7$) declining by half between 42° S and 28° S. The intermediate waters hardly reached those stations closer to the equator so that the increased pCO_2 lowered pH and the saturation of aragonite. A significant fraction of the water column along the Chilean sector of the Humboldt Current System suffers from CO₂-driven compromises to biota, including waters corrosive to calcifying organisms, stress to aerobic organisms or both. The habitat free of CO₂-driven stresses was restricted to the upper mixed layer and to small water parcels at about 1000 m depth. Overall pCO_2 acts as a

hinge connecting respiratory and calcification challenges expected to increase in the future, resulting in a spread of the challenges to aerobic organisms.

1 Introduction

The evolution of the concentrations of atmospheric CO₂ and O₂ over the history of the Earth has played a crucial role in the evolution of life (Dudley, 1998; Berner, 2002). After 800 000 years of relative stability, anthropogenic emissions have driven atmospheric CO₂ to reach 385 ppmv, well above the range of 172–300 ppmv observed over the 800 000 years preceding industrial development (Lüthi et al., 2008), with a dramatic impact in the Earth's climate (Meehl et al., 2007).

Oceans have absorbed almost 50 % of the 7 Gt C yr⁻¹ released by anthropogenic activities (Sabine et al., 2004), and its surface waters now hold approximately 45 μmol kg⁻¹ of CO₂ in excess compared to preindustrial concentrations (Broecker et al., 1985). Increased CO₂ in ocean waters has already lead to a decline of 0.1 units in ocean pH, and may decrease by an additional 0.3 pH units by the end of the century, with a large impact on marine calcifying organisms (Orr et al., 2005; Doney et al., 2009). The thresholds of ocean acidification to marine calcifying organisms are given by the aragonite and calcite saturation values, Ω (Feely et al., 2004;

Orr et al., 2005), with aragonite saturation being more sensitive to ocean acidification than that for calcite. Indeed, calcification processes are already affected at aragonite Ω values <2 (Hauri et al., 2009; Hendriks et al., 2010), although these thresholds are species-specific. Ocean acidification has received considerable attention as the main direct impact of increased ocean CO₂, but other potential impacts of increased CO₂ have been overlooked. Indeed, increased CO₂ and lowered pH also affect respiratory processes by driving reduced binding affinity for oxygen in blood (Pörtner et al., 2004) and a direct ventilatory sensitivity to CO₂ (Burlinson and Smatresk, 2000; McKendry et al., 2001). Hence, increased CO₂ also poses challenges to aerobic respiration, threatening marine life, an impact observed long ago on marine fishes in controlled laboratory conditions (Powers, 1922), and recently addressed by Brewer and Peltzer (2009) in a study of the changing ocean conditions.

Indeed, the efficiency of aerobic respiratory processes depends on the partial pressures of both CO₂ and O₂, which are tightly coupled through the metabolic activity of marine organisms. Brewer and Peltzer (2009) indicated that the efficiency of aerobic respiratory processes is dependent on the ratio of the partial pressures of O₂ and CO₂, which defines the range of conditions compatible with aerobic marine life. Hence, present concerns on the threat posed by on-going declines of marine oxygen in the ocean (Díaz and Rosenberg, 2008; Vaquer-Sunyer and Duarte, 2008; Gilbert et al., 2010) are further aggravated by the parallel increase in CO₂ (Brewer and Peltzer, 2009). Yet, the impacts of hypoxia on marine biota have been traditionally studied in isolation from the effects of increased CO₂. Brewer and Peltzer (2009) highlight the importance of studying the coupled effects of changes in both CO₂ and O₂ on aerobic marine life, based on the notion that elevated dissolved CO₂ concentrations may impose physiological strain and less available energy on marine animals. This results from the fact that hemoglobin has an optimum pH to carry oxygen (Powers, 1922). Hence, these authors use the basic oxidic respiration equation ($C_{\text{org}} + O_2 \rightarrow CO_2$) associated with the free-energy relation ($\Delta G = \Delta G^\circ - RT \cdot \ln[fCO_2]/[C_{\text{org}}][fO_2]$) to derive a Respiration Index (RI), which is used to parametrise the combined effect of O₂ and CO₂ on the efficiency of aerobic respiration. The RI is a simple numerical constraint that is linearly related to available energy, given by the expression:

$$RI \equiv \log_{10} \frac{pO_2}{pCO_2} \quad (1)$$

where $RI \leq 0$ corresponds to the thermodynamic aerobic limit, a formal dead zone; at $RI = 0$ to 0.4 aerobic respiration does not occur; the range $RI = 0.4$ to 0.7 represents the practical limit for aerobic respiration, and the range $RI = 0.7$ to 1.0 delimits the aerobic stress zone. Thus, increased CO₂ aggravates the impacts of hypoxia (Brewer and Peltzer, 2009).

Elevated CO₂ acts as a hinge, connecting two otherwise independent threats to marine life, acidification and hypoxia.

This connection has been poorly studied to date. The areas of the world ocean most sensitive to both these threats are upwelling regions, as they are typically low in oxygen (Grantham et al., 2004) and corrosive to carbonate structures due to high CO₂ levels (Feely et al., 2008).

A particularly vulnerable area is the Humboldt Current System along the Chilean coast, the largest naturally hypoxic area and an important upwelling center (Thiel et al., 2007; Ulloa and Pantoja, 2009), where CO₂, O₂ and pH levels across the water column result from natural variation. In this study we examine the Chilean sector of the Humboldt Current System using data from one single summer cruise, when upwelling is typically strongest and habitat stresses greatest. Whereas the pCO_2 and carbon chemistry in this region has been extensively studied in the past (Torres et al., 2002; Torres et al., 2011), the link between increased CO₂ and hitherto considered independent threats to marine life, ocean acidification and hypoxia has not yet been addressed. Here we provide a first perspective of the latitudinal changes in CO₂-driven compromises to marine life over a distance of 1700 km along a very complex system. We demonstrate how RI and Ω can be used to delineate the water masses where aerobic and calcifying organisms are stressed. Our main objective is to examine, in a predominantly along-shore transect, the connection, through increased CO₂, between challenges to respiration arising from the combination of reduced oxygen values and high pCO_2 levels and challenges to calcification derived from reduced pH levels with high pCO_2 levels. Increased awareness of the connection between compromises to marine biota derived from these two effects of increased CO₂, will hopefully lead to further studies on the seasonal, interannual and long-term trends of the CO₂, O₂ and pH levels.

2 Materials and methods

2.1 Study site

The study was conducted along the Humboldt 2009 cruise on board the R/V *Hespérides* from 5 to 16 March 2009. The cruise track followed the Chilean coast, starting in the Patagonia channels (54.9° S) proceeding North along the Humboldt Current System until Antofagasta (Chile, 23.6° S, Fig. 1). The Humboldt Current System is one of the largest naturally hypoxic areas of the world's oceans (Levin, 2002; Thiel et al., 2007; Ulloa and Pantoja, 2009), characterized by upwelling of cold, oxygen-poor waters supersaturated in CO₂ (Torres et al., 2002). The Humboldt Current System is a quite complex dynamic region, characterized by the presence of a system of along-slope currents that brings waters of both tropical and subpolar origin. The dominant current is the far-offshore equatorward Humboldt Current but near shore a system of poleward and equatorward currents is found, the former formed by the Peru-Chile Counter Current and

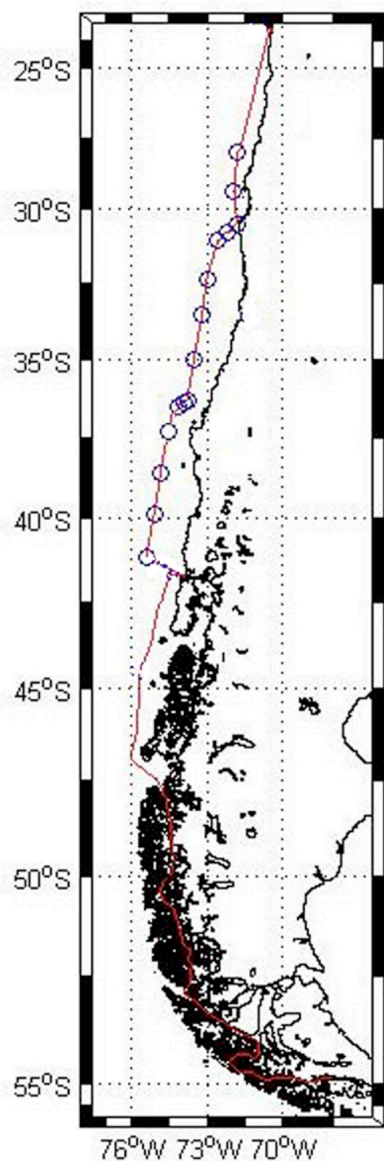


Fig. 1. Cruise track (red line) and sampling stations (blue circles) along the Humboldt Current System (54.9° to 23.6° S).

the near-slope Poleward Undercurrent and the latter by the Peru-Chile Coastal Current (Strub et al., 1998; Silva et al., 2009). The poleward currents are responsible for bringing Subtropical Waters (STW) and Equatorial Subsurface Waters (ESSW) while the equatorward flow brings Subantarctic Waters (SAAW) and Antarctic Intermediate Waters (AAIW). Each of these water masses is characterized by distinct properties, including the levels of CO₂ and O₂.

The Humboldt Current System, and therefore the associated CO₂ and O₂ levels, has substantial interannual and seasonal cycles. Much of the variability in the biogeochemical cycles north of 35° S is directly driven by the interannual ENSO cycle (Halpin et al., 2004). As a result of

warm ENSO events, the Oxygen Minimum Layer (OML) deepens and higher oxygen concentrations in the top 100 m layer are found (Morales et al., 1999). The Humboldt Current System is controlled, to a large extent, by the coastal equatorward winds linked to the Pacific Subtropical Anticyclone. These winds drive all year long coastal upwelling along northern and central Chile, extending to southern Chile in summer. The maximum upwelling-favorable winds occur in summer, the winter-summer difference increasing with latitude. In southern Chile, beyond about 35° S, upwelling only occurs in summer while in winter the polar front provides downwelling-favorable winds (Thiel et al., 2007).

As a result of changes in upwelling most variability occurs in the upper 150 m, therefore, affecting STW and SAAW and, to a lesser degree, ESSW (Blanco et al., 2001; Antezana, 1978); deeper waters, such as AAIW, experience much more moderate seasonal changes, in any case, not directly linked to coastal upwelling. During summer, therefore, we expect there will major near-surface coastal changes associated to the onshore and upward transport of the oxygen-deficient (the Oxygen Minimum Layer, OML) and strongly CO₂ supersaturated tropical and equatorial waters (in surface to reach 100 % near 23° S and 200 % near 30° S) (Torres et al., 2002). The high primary production (PP) values in the upwelling region, particularly intense near several geomorphological coastal features (Strub et al., 1998), strengthens the oxygen-minimum zone and results in CO₂ supersaturated reaching near-surface waters.

2.2 Sampling

A series of 15 stations spaced along the meridional cruise track were sampled. Hydrographic properties were profiled down to 1400 m depth using a Seabird 9 CTD probe. Water samples were collected at different depths (5, 15, 30, 50, 100, 200, 300, 600, 1000, 1400 m) using 12 L Niskin bottles fitted on a Rosette sampler system. Water samples were analyzed for *p*CO₂, O₂, and pH immediately after sampling.

2.3 CO₂ measurements

The partial pressure of CO₂ in the water (*p*CO₂) was measured using a non dispersive infrared gas analyzer (EGM-4, PP systems) that measures *p*CO₂ with a precision of ±1 ppm. For *p*CO₂, near surface water (about 1 m depth) was collected and passed through a gas exchange column (Mini-Module Membrane Contactor) and *p*CO₂ measured, details of this methodology have been described elsewhere (Calleja et al., 2005; Silva et al., 2008).

2.4 O₂ measurements

Oxygen concentration was analysed using high-precision Winkler titration, using a potentiometric electrode and automated endpoint detection (Mettler Toledo, DL28 titrator) (Carpenter, 1965).

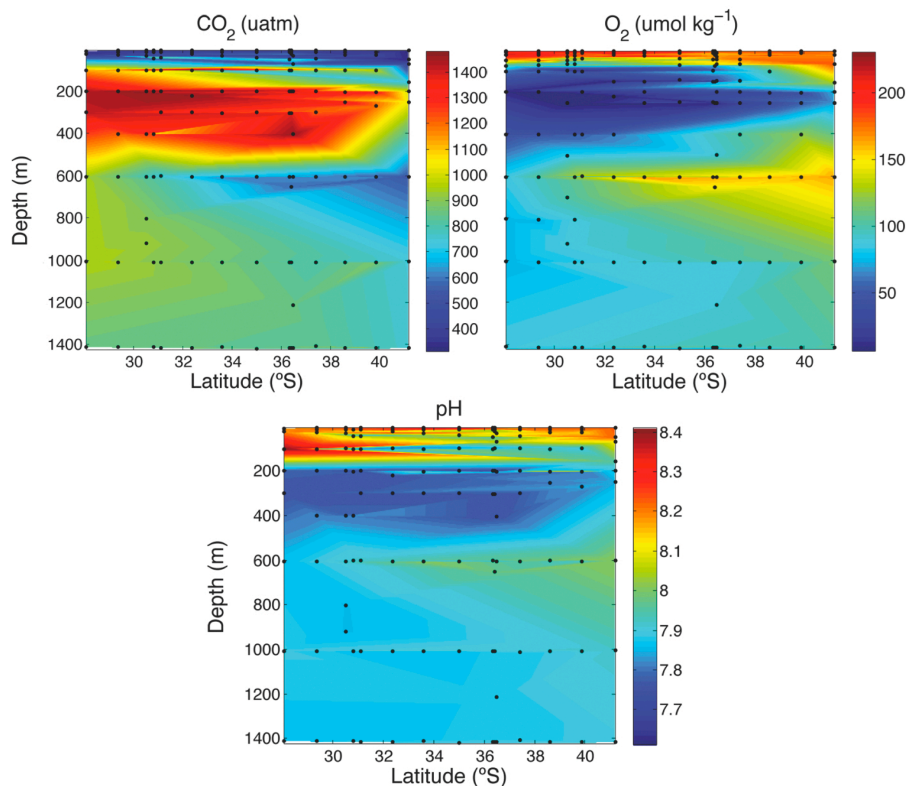


Fig. 2. Contour plots showing the variation in $p\text{CO}_2$, O_2 and pH levels along the studied transect. The black points represent the location of the samples within the water column.

2.5 pH, RI and aragonite saturation (Ω) measurements

All seawater samples for pH, collected immediately after sampling the Niskin bottles for oxygen determinations, were siphoned into 500 mL glass bottles, allowed to overflow and immediately stopped. After temperature stabilization on a water bath at 25 °C, the pH samples were carefully transferred to 10 cm path-length optical glass cells (fitted with a jacket that circulates water at 25 °C) to carry out the double-wavelength spectrophotometric measurements (Clayton and Byrne, 1993). Oxygen concentrations were converted into $p\text{O}_2$ and RI were calculated following Brewer and Peltzer (2009). Ω values for aragonite saturation were calculated from pH, pressure, temperature, salinity and alkalinity using CO₂ SYS (Pierrot et al., 2006). Because the pH- $p\text{CO}_2$ paired couple is not a good predictor of alkalinity, total alkalinity was obtained from the CDIAC data base (Lamb et al., 2001).

3 Results

3.1 Description of water masses and its associated $p\text{CO}_2$, O_2 and pH levels

The ship's meridional transect encompassed waters of equatorial and Antarctic origin, displaying substantial changes in $p\text{CO}_2$ and O_2 . The surface waters, down to 100–150 m, correspond to STW and SAAW, characterized by $p\text{CO}_2$ and O_2 concentrations close to atmospheric equilibrium and by the highest pH values found in the water column (Fig. 2). Immediately below were the hypoxic ESSW, their thickness increasing towards the Equator, where they extend from 100 m to about 300 m depth (Fig. 2). Below this layer and down to about 1000 m we found AAIW, characterized by much higher oxygen concentrations (Fig. 2). The hypoxic ESSW were also characterized by elevated $p\text{CO}_2$ and pH values ($> 1000 \mu\text{atm}$ $p\text{CO}_2$ and < 7.8 pH units, Fig. 2), while the AAIW were characterized by comparatively low $p\text{CO}_2$ and intermediate pH values (Fig. 2). Further below we find the moderately oxygen-depleted Pacific Deep Waters (PDW).

We also present three temperature-salinity diagrams with colour-coded values of the oxygen concentration (Fig. 3a), $p\text{CO}_2$ (Fig. 3b), and pH (Fig. 3c). The oxygen-coded diagram shows interleaving between oxygen-rich AAIW and

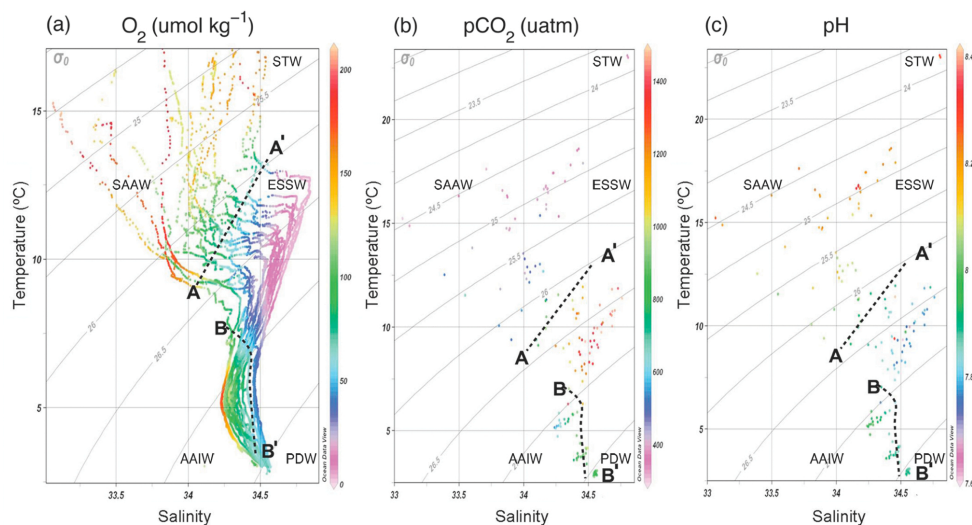


Fig. 3. Temperature-salinity diagram colour-coded for oxygen (a), $p\text{CO}_2$ (b), and pH (c) with potential-density isolines superposed. The dashed lines in (a) illustrate the location of intermediate waters (points denser than defined by line A-A') and their partitioning between waters of Equatorial origin (points above line B-B' and lighter than 27.0) and those of Antarctic origin (points to the left of line B-B'). Deep-water points are found to the right of line B-B' and with densities higher than 27.0. Oxygen values in (a) were derived from the CTD-mounted oxygen sensor calibrated with Winkler analyses from bottle casts, while $p\text{CO}_2$ (b) and pH (c) correspond to the values measured from the bottle casts.

ESSW, with the latter overlaying the former (Fig. 3a). The STW and SAAW surface waters have relatively large oxygen concentrations, with maximum values corresponding to the high-latitude relatively cold SAAW (Fig. 3a). The oxygen-depleted equatorial subsurface waters were also characterized by elevated $p\text{CO}_2$ ($>1000 \mu\text{atm } p\text{CO}_2$; Fig. 3b) and acidic (pH <8.0) waters (Fig. 3c). Indeed, our study area was characterized by a strong negative relationship between $p\text{CO}_2$ and oxygen levels, and between $p\text{CO}_2$ and pH levels, while an opposite relationship was found between oxygen concentrations and pH values (Fig. 4).

3.2 Respiration index and threatened aerobic life

The respiration index, which describes the adequacy of the gaseous composition of the water to maintain aerobic life, reached a minimum at about 200 m depth, with the minimum RI values generally decreasing towards the Equator (Fig. 5). These minimum RI values were below the 0.7 threshold value across most of the region (Fig. 5). The 0.4 and 0.7 RI thresholds were associated with higher CO₂ and lower O₂ values ($\text{O}_2 < 70 \mu\text{mol kg}^{-1}$; Fig. 4a). We examined the contribution of changes in $p\text{CO}_2$ to the observed variability in RI by holding $p\text{CO}_2$ constant at atmospheric equilibrium (Fig. 6a), and calculating the difference between the observed RI and that calculated if $p\text{CO}_2$ was constant (Fig. 6b). This exercise showed that the increased $p\text{CO}_2$ levels in the hypoxic water layer (observed in Fig. 5b) enhance the thickness of the water column that has RI values below the 0.7 threshold, as can be observed in Fig. 6b, and reduces

the RI values of the water column below 100 m by as much as 0.59 RI units at the oxygen minimum zone. Indeed, the thickness of the water column with RI values below the 0.7 threshold increases greatly towards the Equator, encompassing 1/3 of the studied water column at 28° S (Fig. 7a). It is important to emphasize that the pattern described also involves a reduction toward the Equator in the thickness of the upper water layer that presents conditions suitable for aerobic life (RI >0.7), declining by half between 42° S and 28° S (Fig. 7b).

3.3 pH and saturation of aragonite levels as a threat to calcification processes

In addition to reducing the RI values, the increased $p\text{CO}_2$ in intermediate waters also lowers pH and, therefore, the saturation limit for aragonite (Fig. 8a). The aragonite saturation levels may compromise calcification processes ($\Omega < 2$) everywhere in the top 1400 m of the water column except in the uppermost 75 to 125 m, with the thickness of this surface layer increasing from 42° S to 28° S, respectively (Fig. 8b). This pattern is opposite to that observed in RI due to the increase in $p\text{CO}_2$ in the oxygen minimum zone toward the Equator, and the parallel warming of the waters that result in increased saturation levels, by as much as 50 % across the 3 °C meridional gradient encompassed by surface waters.

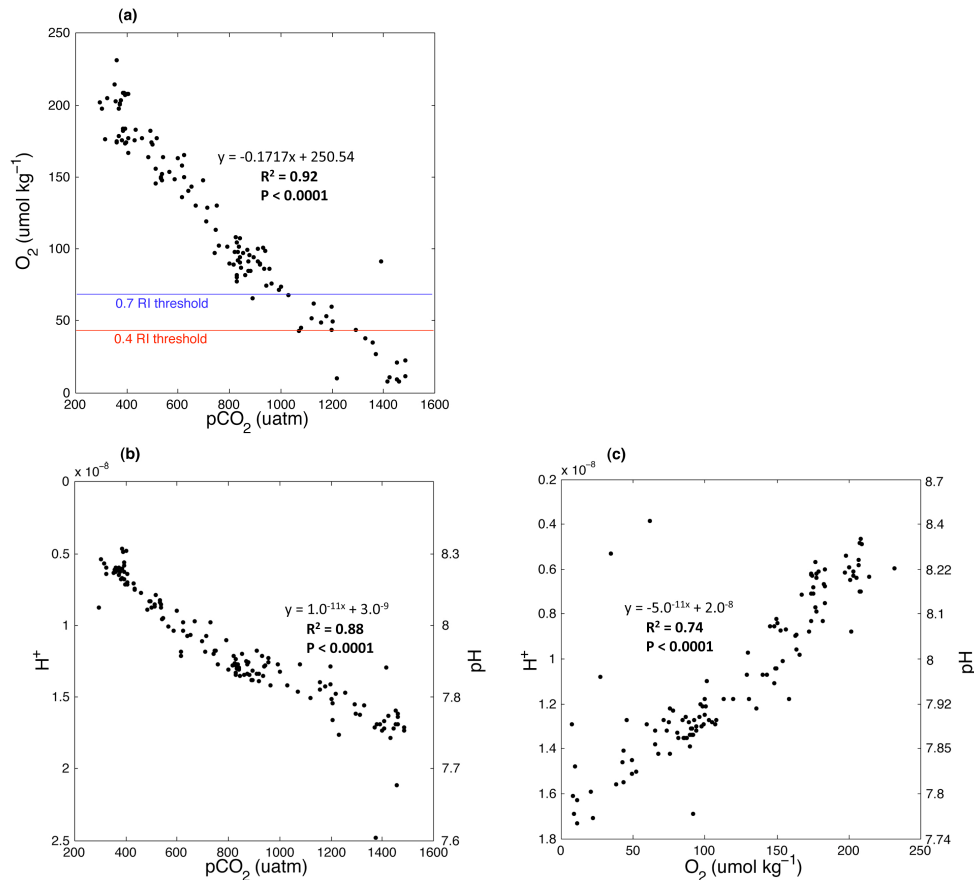


Fig. 4. Relationships between variables: (a) O₂ and pCO₂; (b) H⁺ molar concentration (left axis), pH (right axis) and pCO₂; and (c) H⁺ molar concentration (left axis), pH (right axis) and O₂. The linear regression equations, R^2 and P values are shown.

3.4 Combined threats

The aragonite saturation levels ($\Omega < 2$) were also observed in most of the water column, except in the upper waters and in small scattered water parcels below 600 m. In the northern end of the cruise track the water depths between about 200 and 400 m, corresponding to ESSW, were also associated with RI values (RI < 0.7) that may compromise aerobic respiration (Fig. 9). The thickness of this layer reduced towards the south and almost disappeared in the southern limit of the cruise track. In these waters the aragonite saturation levels were always such that they may also compromise calcification processes ($\Omega < 2$) (Fig. 9).

4 Discussion

The bulk of the water column (0–1400 m) along the Chilean sector of the Humboldt Current System, where summer winds are usually favorable to upwelling events, is strongly acidic or has low RI values which compromise habitat. These waters are associated with the subsurface hypoxic Equatorial

waters that flow South through both the Peru-Chile Counter Current and the Poleward Undercurrent. Compromises are particularly acute for aerobic organisms, as hypoxia rises close to the sea surface (O₂ concentrations < 8 μmol kg⁻¹ at 100 m depth in 30.51° S) towards the north of the study area. pCO₂ levels were also very high (up to 1460 ppm) in association with the hypoxic layer. The negative relationship between CO₂ and O₂ levels is enhanced due to upwelling in this area. The pH values decline in this area, as a typical chemical response to rising CO₂ levels. Therefore, the positive relationship between O₂ and pH is a consequence of the inverse relation with CO₂ (Fig. 4), which is linked to O₂ through metabolic processes and to pH through its role in the seawater carbon buffer system. Indeed, the close relationship between O₂ and pH allows the scaling of two threats, thus far mostly treated as independent, to rising CO₂ levels.

Llanillo et al. (2011) have recently examined the distribution of water masses along the cruise track, in particular the relation between oxygen concentration and the presence of ESSW. These authors found that ESSW are characterized by relatively high salinity and nutrient concentrations, and very

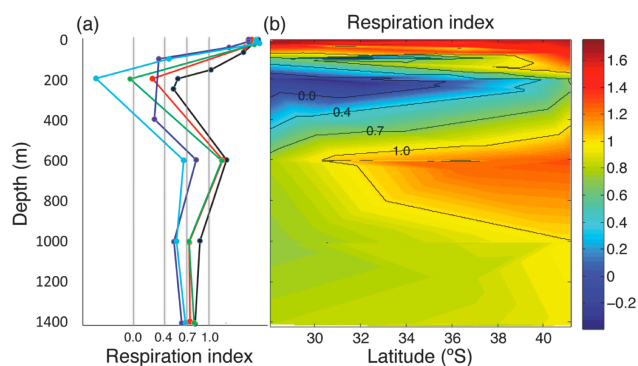


Fig. 5. (a) Vertical profile of RI for five representative stations along the meridional transect (black: station 41.2° S; red: station 37.4° S; green: station 33.6° S; blue: station 30.8° S and light-blue: station 28.03° S). The limits indicated by gray lines correspond to the different thresholds proposed by Brewer and Peltzer (2009): RI \leq 0 corresponds to the thermodynamic aerobic limit, a formal dead zone; RI = 0 to 0.4 aerobic respiration is not observed; RI = 0.4 to 0.7 practical limit for aerobic respiration and RI = 0.7 to 1.0 aerobic stress zone. (b) Contour plot showing the variability in RI along the studied transect.

low oxygen values, leading to an extensive subsurface oxygen minimum zone as reported by previous studies (Fuenzalida et al., 2009; Silva et al., 2009). Llanillo et al. (2011) found that the ESSW, centered at 200–250 m depths, flow poleward progressively losing their identity through mixing with the overlying SAAW and the underlying AAIW until they are no longer recognizable at 41.6° S.

The additional stress to biota in the hypoxic water mass of the Humboldt Current System arising from the high $p\text{CO}_2$ levels has not been discussed earlier. Our results showed that a significant fraction of the water column along the Chilean sector of the Humboldt Current System suffers from CO₂-driven compromises to biota, including corrosive waters to calcifying organisms, stress to aerobic organisms or both. Only those waters shallower than 100 m (STW and SAAW) present conditions free of stress to aerobic organisms (Fig. 9). The threshold imposing challenges to aerobic organisms, as indicated by the RI values and particularly by RI < 0.7, was associated with O₂ values below 70 $\mu\text{mol kg}^{-1}$. This value is slightly higher than the typical threshold for hypoxia (Gray et al., 2002), but is consistent with experimental evidence that yields a median lethal oxygen concentration among studied taxa start at 60 $\mu\text{mol L}^{-1}$, while the hypoxic threshold for the most resistant organisms is 25 $\mu\text{mol L}^{-1}$ (Vaquer-Sunyer and Duarte, 2008; Keeling et al., 2010). This challenge is highly increased by consideration of the increased $p\text{CO}_2$ levels, which lowered the RI value by up to 0.59 RI units and increased the thickness of the water column with RI < 0.7. Hence, our results concur with those of Brewer and Peltzer (2009) to suggest that increased $p\text{CO}_2$ levels aggravate the

challenges to aerobic organisms in oxygen deficient waters, such as those in the Humboldt Current System.

Whereas our study represents a quasi-synoptic assessment of the extent of challenges derived from $p\text{CO}_2$, and associated pH levels, and O₂ in the water column of the Humboldt Current System, these were expected to be highly dynamic. The oxygen minimum of the Humboldt Current System shows seasonal and interannual variability, driven by upwelling events and large-scale perturbations in regional circulation, such as those accompanying El Niño events. The oxygen content in the top 100 m layer is higher in the region during El Niño events (Morales et al., 1999; Ulloa et al., 2001). In addition to seasonal and interannual oscillations, the CO₂-driven challenges to biota reported here are expected to increase in the future. Atmospheric $p\text{CO}_2$ levels are expected to reach 700 to 1000 ppm by the end of the 21st Century (Meehl et al., 2007), with an increase in $p\text{CO}_2$ at depth more than 1000 μatm in the Pacific (Brewer and Peltzer, 2009), resulting in a spread of the respiratory challenges to aerobic organisms. The corresponding pH levels are expected to continue to decline, being reduced by 0.3 units below present values by the end of the 21st Century and by up to 0.7 units by 2300 (Caldeira and Wickett, 2003; Doney et al., 2009). In addition, oxygen concentrations are declining in many areas of the ocean (Stramma et al., 2008; Keeling et al., 2010), further affecting the RI ratio.

The area where biocalcification processes may be close to being compromised can be delineated from the water column with saturation levels, Ω for aragonite < 2 (cf. Orr et al., 2005; Yates and Halley, 2006; Guinotte and Fabry, 2008; Hauri et al., 2009; Hendriks et al., 2010), which encompasses most of the water column except for the upper layer (above 70 m). The thickness of the water column where biocalcification processes may be impacted is largest at mid-latitudes (between about 30 and 37° S) and decreases slowly towards high latitudes and rapidly towards the Equator. This swift change in the equatorial region is opposite to what happens to the layer where aerobic respiration is compromised. The pre-industrial conditions (CO₂ level of around 260–270 ppmv (Wigley, 1983), and ocean temperatures approximately 1 °C lower than at present (Hughes, 2000)) suggest that Ω for aragonite in the surface of the ocean could have been 0.2 units higher than present (calculations not shown). Reduced aragonite saturation levels and RI, are driven by $p\text{CO}_2$, each includes a second, independent, driver: temperature in the case of biocalcification and oxygen concentration in the case of aerobic respiration. $p\text{CO}_2$ acts, therefore, as a hinge connecting respiratory and calcification challenges.

In summary, ocean acidification affects most waters below 150 m, while respiratory compromises are located within the 200 to 400 m layer (Fig. 9). These two challenges show similar trends at mid and high latitudes but have opposite trends within equatorial waters. The whole cruise track carried out in summer was influenced by upwelling, but yet the temperature displayed a significant latitudinal gradient at all depths.

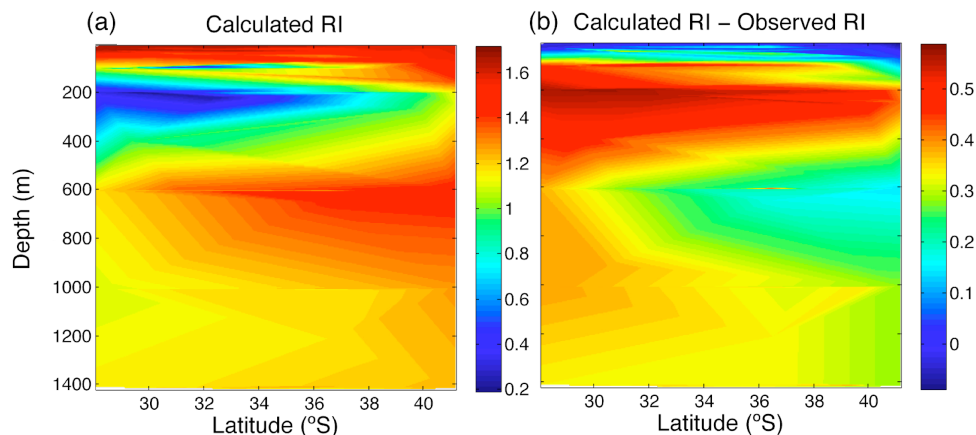


Fig. 6. Contour plot showing the distribution of (a) the calculated RI assuming a constant $p\text{CO}_2$ in atmospheric equilibrium ($385 \mu\text{atm}$) and (b) the difference between the calculated RI and that observed along the studied transect.

This clearly must have affected the chemical processes in the water column, as for example the O₂ solubility, which increases with lower temperatures (Keeling et al., 2010). In general, the subsurface depth layer is affected by biocalcification and hypoxia, its thickness being maximum at low latitudes (200 to 400 m) and decreasing to nearly zero at high latitudes (Fig. 9), which is consistent with the increase of the ESSW thickness towards the Equator and in summer (Blanco et al., 2001). The habitat free of CO₂-driven stresses was restricted to the upper mixed layer and to small water parcels at about 1000 m depth (Fig. 9). Increased $p\text{CO}_2$ in the future may increase the thickness of the water column with both RI and aragonite saturation reaching values under the threshold that compromises marine life, therefore, compressing the vertical extent of the stress-free habitat.

Probably, both the aragonite saturation threshold for biocalcification and the threshold RI affecting respiration vary across taxa (cf. Hendriks et al., 2010 and Vaquer-Sunyer and Duarte, 2008, respectively), depending on their metabolic capacities. Indeed, whereas most metazoans are excluded from the oxygen minimum zone of the Humboldt Current System, specialized crustacean communities, including copepods and euphasids, have been reported to enter this hypoxic layer (Escribano et al., 2009). The temperature also is a factor that may lead to a differentiated biological resistance to the RI threshold. Higher temperatures are mostly associated with higher metabolic rates and respiration (Doney et al., 2012). Therefore, organisms affected by the same RI value could be more stressed in the North of Chile. Use of the RI value as a predictive tool to evaluate and project the impact of increased $p\text{CO}_2$ on aerobic organisms in this region requires, therefore, experimental evidence of the RI thresholds for aerobic respiration of the main taxa in the ecosystem.

The most intense upwelling in Chile takes place near small capes and bays, where subsurface waters are exported offshore by ~ 125 km (Fonseca and Farias, 1987).

These upwelling centers are the site for major fisheries, with catches that represent 40% of the annual landings of the Humboldt Current System (Thiel et al., 2007). Along the Humboldt Current System about 40 important commercial species of fishes, crustaceans, molluscs, echinoderms and seaweeds are found (Montecino and Lange, 2009). Our study showed that the extent of the threats toward the surface layer is presumably larger towards the coast when deep upwelling events, reaching ESSW layers, are most intense. These events could lead to RI and Ω values closer to the threshold values that compromise marine life, therefore possibly affecting the large fisheries supported at these sites. Additionally, events associated with changes in temperature and O₂ levels, such as El Niño, have been extremely adverse on anchovy and positive on sardine populations (Alheit and Bernal, 1993). It is likely that these events are also associated with concurrent changes in CO₂ levels, leading to a compression of the habitat suitable for aerobic organisms.

Pörtner and Langenbuch (2005) have described mechanisms of short and long-term sensitivity to CO₂ in fish and have shown how elevated CO₂ levels, particularly when combined with other factors, may become a life risk for different organisms. The trends towards increased $p\text{CO}_2$ and reduced O₂ concentrations in the future may compress the water column available for aerobic organisms and expand the minimum oxygen zone until zones where fisheries species, such as the Humboldt squid and fish species, are located.

5 Conclusions

In this study we presented the risk for aerobic and calcifying marine organisms associated to high $p\text{CO}_2$ and low O₂ levels. The study was centered in an area naturally low in oxygen and with high $p\text{CO}_2$ levels, potentially corrosive to carbonate structures. The main point of this manuscript is to

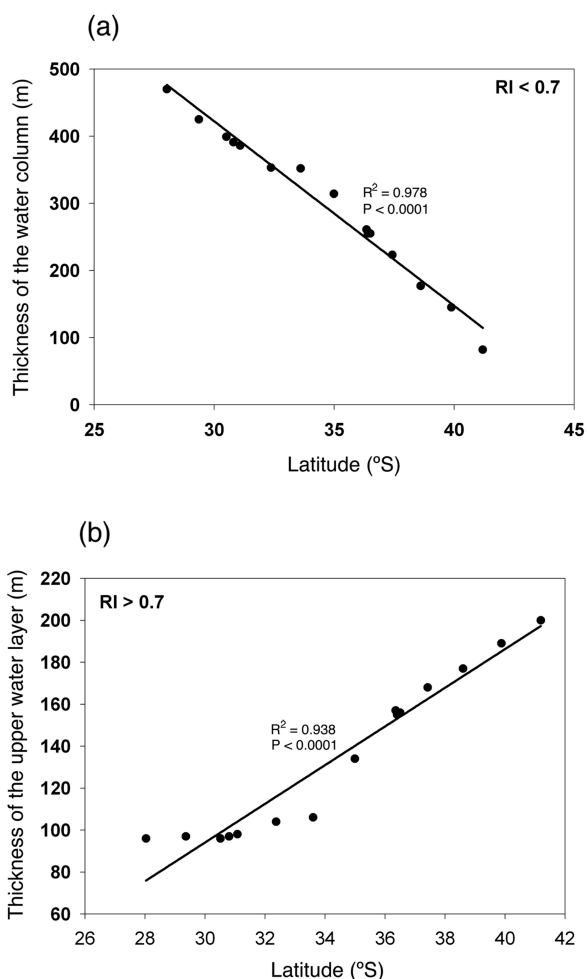


Fig. 7. Relationships between the thickness of the water column and latitude: (a) RI < 0.7 in the top 1400 m; (b) RI > 0.7 in the top 200 m.

examine the co-variation between $p\text{CO}_2$ and O_2 to explore how ocean acidification and hypoxia trends are not independent threats, but are connected to one another through the effect of CO_2 on both respiratory activity and calcification rates. With this purpose we extended the thermodynamic model of Brewer and Peltzer (2009) on joint effects of $p\text{CO}_2$ and O_2 on respiration to also address the effects of $p\text{CO}_2$, pH and calcification. With the definition of the RI index (respiration index) and saturation states of aragonite, we have attempted to delineate water masses in the Humboldt Current System where respiration and calcification may be compromised.

This study can be used as a predictive model of the future situation that oceans are likely to exhibit, when considering the expected trends in the evolution of both O_2 and $p\text{CO}_2$ levels. Relating $p\text{CO}_2$ and O_2 values by means of the respiration index is key in understanding the dimension of the threat that aerobic organisms are faced with. The distribution

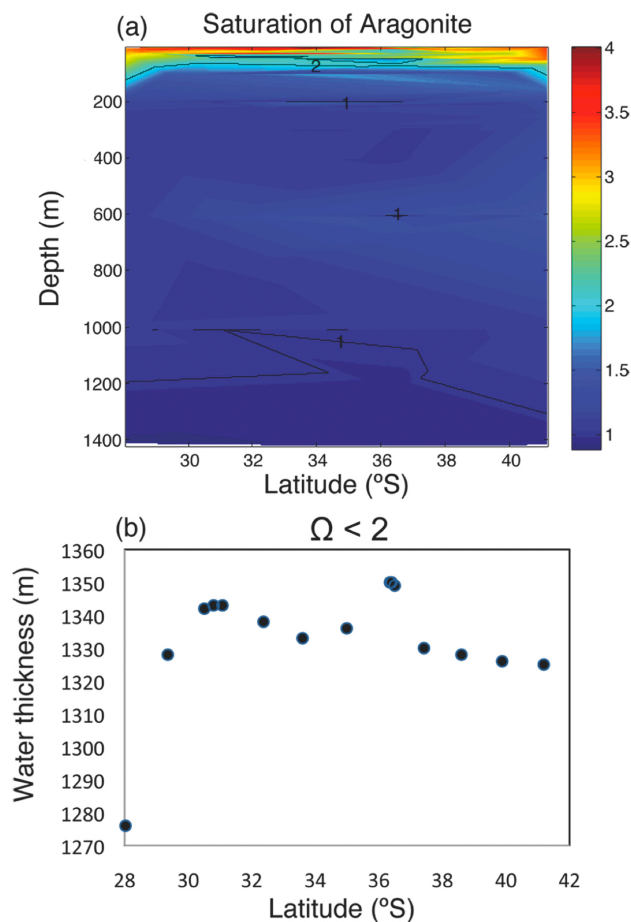


Fig. 8. (a) Contour plot showing the distribution of aragonite saturation index (Ω), where the limits indicated by gray lines correspond to the thresholds of aragonite saturation ($\Omega = 1$ and 2). (b) Thickness of the water column with $\Omega < 2$ along the studied transect.

of this index indeed shows that high $p\text{CO}_2$ contributes to exacerbate the challenges to respiration in Humboldt Current System. As well as this respiratory threat, it is also necessary to take into account the stress inflicted upon calcifying processes, associated with increased $p\text{CO}_2$ levels, resulting in decreased pH levels and low saturation levels Ω for aragonite, where calcification may be compromised. The RI and the saturation state of aragonite have been used in this work as predictive tools to evaluate and project the impact of increased $p\text{CO}_2$ on aerobic and calcifying organisms, showing that along the Chilean sector of the Humboldt Current System the habitat free of CO_2 -driven stresses was restricted to the upper mixed layer and to small water parcels at about 1000 m depth.

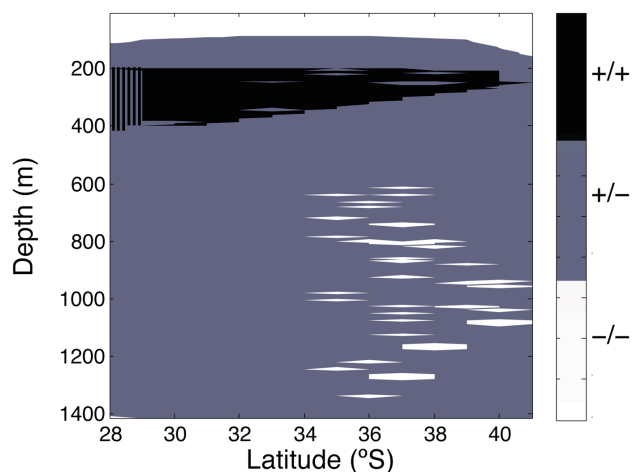


Fig. 9. Distribution of compromises (biocalcification compromised, $\Omega < 2$; aerobic respiration compromised, $RI < 0.7$) to marine life along the studied transect. ++ = both biocalcification and respiration compromised; +/- = only biocalcification compromised; -/- = no compromises. The missing combination (-/+ = only respiration compromised) was not observed. Note that the 28° station had data only at 200 and 600 m depths, therefore, the region with compromises to both biocalcification and respiration was likely missed by the data; this region is hatched with vertical lines.

Table 1. Depth, position and distance to the coast for each station.

N° station	Depth (m)	Latitude (° S)	Longitude (° W)	Distance coast (km)
1	1400	41.19	75.41	123
2	1400	39.88	75.09	118
3	1400	38.6	74.82	113
4	1400	37.42	74.41	65
5	1400	36.5	74.14	90
6	1400	36.4	73.91	74
7	1400	36.35	73.78	66
8	1400	34.99	73.51	102
9	1400	33.6	73.51	151
10	1400	32.37	73.00	138
11	1400	31.08	72.57	86
12	1400	30.8	72.20	47
13	912	30.51	71.81	11
14	1400	29.36	71.92	46
15	1400	28.03	71.79	63

Acknowledgements. This is a contribution to the Humboldt-2009 project, funded by the Spanish Ministry of Science and Innovation (ref. CTM2009-02497-E/MA) and was also supported by funding from the LINCGlobal (PUC-CSIC). We thank the cruise participants, UTM technicians, crew and commander of R/V

Hespérides for help during the cruise. We thank E. T. Peltzer, F. Millero and P. Llanillo for assistance with calculations. E. M. was supported by a JAE fellowship from CSIC.

Edited by: K. Suzuki

References

- Alheit, J. and Bernal, P.: Effects of physical and biological changes on the biomass yield of the Humboldt current system, Large Marine Ecosystems, Am. Assoc. Adv. Sci. Press, Washington DC, 53–68, 1993.
- Antezana, T.: Distribution of Euphausiids in the Chile-Peru current with particular reference to the endemic *Euphausia mucronata* and oxygen minima layer, Ph.D. Thesis, University of California, 1978.
- Berner, R. A.: Examination of hypotheses for the Permo-Triassic boundary extinction by carbon cycle modeling, P. Natl. Acad. Sci. USA, 99, 4172–4177, doi:10.1073/pnas.032095199, 2002.
- Blanco, J. L., Thomas, A. C., Carr, M.-E., and Strub P. T.: Seasonal climatology of hydrographic conditions in the upwelling region off northern Chile, J. Geophys. Res., 106, 11451–11467, 2001.
- Brewer, P. G. and Peltzer, E. T.: Limits to marine life, Science, 321, 347–348, doi:10.1126/science.1170756, 2009.
- Broecker, W. S., Takahashi, T., and Peng, T.-H.: Reconstruction of the past atmospheric CO₂ contents of the contemporary ocean: an evaluation, Technical Report, 1985.
- Burleson, M. L. and Smatresk, N. J.: Branchial chemoreceptors mediate ventilatory response to hypercapnic acidosis in channel catfish, Comp. Biochem. Phys. A., 125, 403–414, doi:10.1016/S1095-6433(00)00167-7, 2000.
- Caldeira, K. and Wickett, M. E.: Anthropogenic carbon and ocean pH, Nature, 425, 365, 2003.
- Calleja, M. L., Duarte, C. M., Navarro, N., and Agustí, S.: Control of air-sea CO₂ disequilibria in the subtropical NE Atlantic by planktonic metabolism under the ocean skin, Geophys. Res. Lett., 32, L08606, doi:10.1029/2004GL022120, 2005.
- Carpenter, J. H.: The accuracy of the Winkler method for dissolved oxygen analysis, Limnol. Oceanogr., 10, 135–140, 1965.
- Clayton, T. D. and Byrne, R. H.: Spectrophotometric seawater pH measurements: total hydrogen ion concentration scale calibration of m-cresol purple and at-sea results, Deep-Sea Res. Pt. I., 40, 2115–2129, doi:10.1016/0967-0637(93)90048-8, 1993.
- Diaz, R. J. and Rosenberg, R.: Spreading dead zones and consequences for marine ecosystems, Science, 321, 926–929, doi:10.1126/science.1156401, 2008.
- Doney, S. C., Fabry, V. J., Feely, R. A., and Kleypas, J. A.: Ocean acidification: the other CO₂ problem, Annu. Rev. Mar. Sci., 1, 169–192, doi:10.1146/annurev.marine.010908.163834, 2009.
- Doney, S. C., Ruckelshaus, M., Duffy, J. E., Barry, J. P., Chan, F., English, C. A., Galindo, H. M., Grebmeier, J. M., Hollowed, A. B., Knowlton, N., Polovina, J., Rabalais, N. N., Sydeman, W. J., and Talley, L. D.: Climate change impacts on marine ecosystems, Annu. Rev. Mar. Sci., 4, 4.1–4.27, doi:10.1146/annurev-marine-041911-111611, 2012.
- Dudley, R.: Atmospheric oxygen, giant paleozoic insects and the evolution of aerial locomotor performance, J. Exp. Biol., 201, 1043–1050, 1998.

- Escribano, R., Hidalgo, P., and Krautz, C.: Zooplankton associated with the oxygen minimum zone system in the northern upwelling region of Chile during march 2000, *Deep-Sea Res. Pt. II*, 56, 1083–1094, doi:10.1016/j.dsr2.2008.09.009, 2009.
- Feely, R. A., Sabine, C. L., Lee, K., Berelson, W., Kleypas, J., Fabry, V. J., and Millero, F. J.: Impact of anthropogenic CO₂ on the CaCO₃ system in the oceans, *Science*, 305, 362–366, doi:10.1126/science.1097329, 2004.
- Feely, R. A., Sabine, C. L., Hernandez-Ayon, J. M., Ianson, D., and Hales, B.: Evidence for upwelling of corrosive “acidified” water onto the continental shelf, *Science*, 320, 1490–1492, doi:10.1126/science.1155676, 2008.
- Fonseca, T. and Farías, M.: Estudio del proceso de surgencia en la costa chilena utilizando percepción remota, *Investigación Pesquera (Chile)*, 34, 33–46, 1987.
- Fuenzalida, R., Schneider, W., Garcés-Vargas, J., Bravo, L., and Lange, C.: Vertical and horizontal extension of the oxygen minimum zone in the eastern South Pacific Ocean, *Deep-Sea Res. Pt. II*, 56, 992–1003, doi:10.1016/j.dsr2.2008.11.001, 2009.
- Gilbert, D., Rabalais, N. N., Díaz, R. J., and Zhang, J.: Evidence for greater oxygen decline rates in the coastal ocean than in the open ocean, *Biogeosciences*, 7, 2283–2296, doi:10.5194/bg-7-2283-2010, 2010.
- Grantham, B. A., Chan, F., Nielsen, K. J., Fox, D. S., Barth, J. A., Huyer, A., Lubchenco, J., and Menge, B. A.: Upwelling-driven nearshore hypoxia signals ecosystem and oceanographic changes in the northeast Pacific, *Nature*, 429, 749–754, doi:10.1038/nature02605, 2004.
- Gray, J. S., Wu, R. S. S., and Or, Y. Y.: Effects of hypoxia and organic enrichment on the coastal marine environment, *Mar. Ecol.-Prog. Ser.*, 238, 249–79, 2002.
- Guinotte, J. M. and Fabry, V. J.: Ocean acidification and its potential effects on marine ecosystems, *Ann. NY Acad. Sci.*, 1134, 320–342, doi: 10.1196/annals.1439.013, 2008.
- Halpin, P. M., Strub, P. T., Peterson, W. T., and Baumgartner, T. R.: An overview of interactions among oceanography, marine ecosystems, climatic and human disruptions along the eastern margins of the Pacific Ocean, *Rev. Chil. Hist. Nat.*, 77, 371–409, 2004.
- Hauri, C., Gruber, N., Plattner, G.-K., Alin, S., Feely, R. A., Hales, B., and Wheeler, P. A.: Ocean acidification in the California Current System, *Oceanography*, 22, 58–69, doi:10.5670/oceanog.2009.97, 2009.
- Hendriks, I. E., Duarte, C. M., and Álvarez, M.: Vulnerability of marine biodiversity to ocean acidification: a meta-analysis, *Estuar, Coast. Shelf S.*, 86, 157–164, doi:10.1016/j.ecss.2009.11.022, 2010.
- Hughes, L.: Biological consequences of global warming: is the signal already, *Trends Ecol. Evol.*, 15, 56–61, doi:10.1016/S0169-5347(99)01764-4, 2000.
- Keeling, R. F., Körtzinger, A., and Gruber, N.: Ocean deoxygenation in a warming world, *Annual Review of Marine Science*, 2, 199–229, doi:10.1146/annurev.marine.010908.163855, 2010.
- Lamb, M. F., Sabine, C. L., Feely, R. A., Wanninkhof, R., Key, R. M., Johnson, G. C., Millero, F. J., Lee, K., Peng, T.-H., Kozyr, A., Bullister, J. L., Greeley, D., Byrne, R. H., Chipman, D. W., Dickson, A. G., Goyet, C., Guenther, P. R., Ishii, M., Johnson, K. M., Keeling, C. D., Ono, T., Shitashima, K., Tilbrook, B., Takahashi, T., Wallace, D. W. R., Watanabe, Y. W., Winn, C., and Wong, C. S.: Consistency and synthesis of Pacific Ocean CO₂ survey data, *Deep Sea Res. Pt. II*, 49, 21–58, doi:10.1016/S0967-0645(01)00093-5, 2001.
- Levin, L. A.: Deep-ocean life where oxygen is scarce, *Am. Sci.*, 90, 436–444, 2002.
- Llanillo, P., Pelegr, J. L., Duarte, C. M., Emelianov, M., Gasser, M., Gourrion, J., and Rodríguez-Santana, A.: Meridional and zonal changes in water properties along the continental slope off central and northern Chile, *Cienc. Mar.*, 38(2B), in press, 2012.
- Lüthi, D., Le Floch, M., Bereiter, B., Blunier, T., Barnola, J. M., Siegenthaler, U., Raynaud, D., Jouzel, J., Fischer, H., Kawamura, K., and Stocker, T. F.: High-resolution carbon dioxide concentration record 650 000–800 000 years before present, *Nature*, 453, 379–382, doi:10.1038/nature06949, 2008.
- McKendry, J. E., Milsom, W. K., and Perry, S. F.: Branchial CO₂ receptors and cardiorespiratory adjustments during hypercarbia in Pacific spiny dogfish (*Squalus acanthias*), *J. Exp. Biol.*, 204, 1519–1527, 2001.
- Meehl, G. A., Stocker, T. F., Collins, W. D., Friedlingstein, P., Gaye, A. T., Gregory, J. M., Kitoh, A., Knutti, R., Murphy, J. M., Noda, A., Raper, S. C. B., Watterson, I. G., Weaver, A. J., and Zhao, Z.-C.: Global climate projections, in: *climate change 2007: the physical science basis. Contribution of working group I to the fourth assessment report of the intergovernmental panel on climate change*, edited by: Solomon, S., Qin, D., Manning, M., Chen, Z., Marquis, M., Averyt, K. B., Tignor, M., and Miller, H. L., Cambridge University Press, Cambridge, United Kingdom and New York, NY, USA, 2007.
- Montecino, V. and Lange, C. B.: The Humboldt Current System: Ecosystem components and processes, fisheries, and sediment studies, *Prog. Oceanogr.*, 83, 65–79, doi:10.1016/j.pocean.2009.07.041, 2009.
- Morales, C. E., Hormazábal, S. E., and Blanco, J. L.: Interannual variability in the mesoscale distribution of the depth of the upper boundary of the oxygen minimum layer off northern Chile (18–24S): implications for the pelagic system and biogeochemical cycling, *J. Mar. Res.*, 57, 909–932, 1999.
- Orr, J. C., Fabry, V. J., Aumont, O., Bopp, L., Doney, S. C., Feely, R. A., Gnanadesikan, A., Gruber, N., Ishida, A., Joos, F., Key, R. M., Lindsay, K., Maier-Reimer, E., Matear, R., Monfray, P., Mouchet, A., Najjar, R. G., Plattner, G.-K., Rodgers, K. B., Sabine, C. L., Sarmiento, J. L., Schlitzer, R., Slater, R. D., Totterdell, I. J., Weirig, M.-F., Yamanaka, Y., and Yool, A.: Anthropogenic ocean acidification over the twenty-first century and its impact on calcifying organisms, *Nature*, 437, 681–686, doi:10.1038/nature04095, 2005.
- Pierrot, D., Lewis, E., and Wallace, D. W. R.: MS Excel program developed for CO₂ system calculations. ORNL/CDIAC-105A. Carbon dioxide information analysis center, Oak Ridge National Laboratory, U.S., Department of Energy, Oak Ridge, Tennessee, 2006.
- Pörtner, H. O. and Langenbuch, M.: Synergistic effects of temperature extremes, hypoxia, and increases in CO₂ on marine animals: from Earth history to global change, *J. Geophys. Res.*, 110, C09S10, doi:10.1029/2004JC002561, 2005.
- Pörtner, H. O., Langenbuch, M., and Reipschläger, A.: Biological impact of elevated ocean CO₂ concentrations: lessons from animal physiology and Earth history, *J. Oceanogr.*, 60, 705–718, doi: 10.1007/s10872-004-5763-0, 2004.

- Powers, E. B.: The physiology of the respiration of fishes relation to the hydrogen ion concentration of the medium, *J. Gen. Physiol.*, 4, 305–317, 1922.
- Sabine, C. L., Feely, R. A., Gruber, N., Key, R. M., Lee, K., Bullister, J. L., Wanninkhof, R., Wong, C. S., Wallace, D. W. R., Tilbrook, B., Millero, F. J., Peng, T.-H., Kozyr, A., Ono, T., and Rios, A. F.: The oceanic sink for anthropogenic CO₂, *Science*, 305, 367–371, doi: 10.1126/science.1097403, 2004.
- Silva, J., Feijóo, P., and Santos, R.: Underwater measurements of carbon dioxide evolution in marine plant communities: a new method, *Estuar. Coast. Shelf S.*, 78, 827–830, doi:10.1016/j.ecss.2008.02.019, 2008.
- Silva, N., Rojas, N., and Fedele, A.: Water masses in the Humboldt Current System: properties, distribution, and the nitrate deficit as a chemical water mass tracer for Equatorial Subsurface Water off Chile, *Deep-Sea Res. Pt. II*, 56, 1004–1020, doi:10.1016/j.dsr2.2008.12.013, 2009.
- Stramma, L., Johnson, G. C., Sprintall, J., and Mohrholz, V.: Expanding oxygen-minimum zones in the Tropical Oceans, *Science*, 320, 655–658, doi: 10.1126/science.1153847, 2008.
- Strub P. T., Mesías, J. M., Montecino, V., Rutllant, J., and Salinas, S.: Coastal ocean circulation off western South America, *The sea*, 11, 273–313, 1998.
- Thiel, M., Macaya, E. C., Acuna, E., Arntz, W. E., Bastias, H., Brokordt, K., Camus, P. A., Castilla, J. C., Castro, L. R., Cortes, M., Dumont, C. P., Escribano, R., Fernandez, M., Gajardo, J. A., Gaymer, C. F., Gomez, I., Gonzalez, A. E., Gonzalez, H. E., Haye, P. A., Illanes, J.-E., Iriarte, J. L., Lancellotti, D. A., Luna-Jorquera, G., Luxoro, C., Manriquez, P. H., Marin, V., Munoz, P., Navarrete, S. A., Perez, E., Poulin, E., Sellanes, J., Hito Sepulveda, H., Stotz, W., Tala, F., Thomas, A., Vargas, C. A., Vasquez, J. A., and Vega, J. M. A.: The Humboldt Current System of northern and central Chile: oceanographic processes, ecological interactions and socioeconomic feedback, *Oceanogr. Mar. Biol.*, 45, 195–344, 2007.
- Torres, R., Turner, D., Rutllant, J., Sobarzo, M., Antezana, T., and Gonzalez, H. E.: CO₂ outgassing off central Chile (31–30° S) and northern Chile (24–23° S) during austral summer 1997: the effect of wind intensity on the upwelling and ventilation of CO₂-rich waters, *Deep-Sea Res. Pt. I*, 49, 1413–1429, doi:10.1016/S0967-0637(02)00034-1, 2002.
- Torres, R., Pantoja, S., Harada, N., González, H. E., Daneri, G., Frangopulos, M., Rutllant, J. A., Duarte, C. M., Rúaiz-Halpern, S., Mayol, E., and Fukasawa, M.: Air-sea CO₂ fluxes along the coast of Chile: From CO₂ outgassing in central northern upwelling waters to CO₂ uptake in southern Patagonian fjords, *J. Geophys. Res.*, 116, C09006, doi:10.1029/2010JC006344, 2011.
- Ulloa, O. and Pantoja, S.: The oxygen minimum zone of the eastern South Pacific, *Deep-Sea Res. Pt. II*, 56, 987–991, doi:10.1016/j.dsr2.2008.12.004, 2009.
- Ulloa, O., Escribano, R., Hormazabal, S., Quiñones, R. A., González, R. R., and Ramos, M.: Evolution and biological effects of the 1997–98 El Niño in the upwelling ecosystem off northern Chile, *Geophys. Res. Lett.*, 28, 1591–1594, doi:10.1029/2000GL011548, 2001.
- Vaquer-Sunyer, R. and Duarte, C. M.: Thresholds of hypoxia for marine biodiversity, *P. Natl. Acad. Sci. USA*, 105, 15452–15457, doi: 10.1073/pnas.0803833105, 2008.
- Wigley, T. M. L.: The pre-industrial carbon dioxide level, *Climatic Change*, 5, 315–320, doi:10.1007/BF02423528, 1983.
- Yates, K. K. and Halley, R. B.: CO₃²⁻ concentration and pCO₂ thresholds for calcification and dissolution on the Molokai reef flat, Hawaii, *Biogeosciences*, 3, 357–369, doi:10.5194/bg-3-357-2006, 2006.